NRC Publications Archive
Archives des publications du CNRC

Use of silicone membranes to enhance gas transfer during microbial fuel cell operation on carbon monoxide
Hussain, A.; Tartakovsky, B.; Guiot, S. R.; Raghavan, V.

National Research Council Canada   Conseil national de recherches Canada

Canada

Use of silicone membranes to enhance gas transfer during microbial fuel cell operation on carbon monoxide

A. Hussain [a,b,*], B. Tartakovsky [a], S.R. Guiot [a], V. Raghavan [b]

[a] Biotechnology Research Institute, National Research Council of Canada, 6100 Royalmount Ave., Montreal, QC, Canada H2P 2R2
[b] Department of Bioresource Engineering, McGill University, Ste-Anne-de-Bellevue, QC, Canada H9X 3V9

ARTICLE INFO

ABSTRACT

Electricity generation in a microbial fuel cell (MFC) using carbon monoxide (CO) or synthesis gas (syngas) as a carbon source has been demonstrated recently. A major challenge associated with CO or syngas utilization is the mass transfer limitation of these sparingly soluble gases in the aqueous phase. This study evaluated the applicability of a dense polymer silicone membrane and thin wall silicone tubing for CO mass transfer in MFCs. Replacing the sparger used in our previous study with the membrane systems for CO delivery resulted in improved MFC performance and CO transformation efficiency. A power output and CO transformation efficiency of up to 18 mW L_R^{-1} (normalized to anode compartment volume) and 98%, respectively, was obtained. The use of membrane systems offers the advantage of improved mass transfer and reduced reactor volume, thus increasing the volumetric power output of MFCs operating on a gaseous substrate such as CO.

1. Introduction

Biomass represents a significant source of renewable energy (Song, 2002). The gasification of biomass at high temperatures leads to the production of synthesis gas (syngas), which mainly consists of carbon monoxide (CO) and hydrogen (H_2). Syngas can be converted to liquid (ethanol, methanol, butanol, etc.) or gaseous (H_2, methane) fuels by catalytic or microbial conversion (Henstra et al., 2007; Munasinghe and Khanal, 2010a; Sipma et al., 2006). Syngas produced by partial oxidation using air, has a varying composition and a low heating value. It is often utilized for electricity generation by internal combustion (Bridgwater, 2006), however the efficiency of the internal combustion generators is relatively low. Direct conversion of syngas to electricity in a fuel cell offers a cleaner and a more efficient process for electricity generation. However, fuel cells are sensitive to the changes in the syngas composition (Kim and Chang, 2009; Song, 2002) and impurities such as sulfur. For examples, solid oxide fuel cells are particularly sensitive to sulfur compounds, with >1 ppm sulfur leading to irreversible poisoning of the anode.

As an alternative, syngas could be converted to electricity in a microbial fuel cell (MFC) (Kim and Chang, 2009; Mehta et al., 2010). This process relies on the ability of an anaerobic consortium of electricigenic and carboxydotrophic microorganisms to produce electricity from CO and H_2. Such an MFC-based process might offer several advantages such as a high transformation efficiency, a broad range of operating conditions, high bio-catalytic activity and considerable resistance to poisoning by fuel impurities (Kim and Chang, 2009; Mehta et al., 2010).

Kim and Chang (2009) demonstrated electricity generation from CO in a two-stage reactor system, in which the CO was first microbiologically converted to fermentation products and then the products were fed to the second reactor (MFC). Instead of a two-stage process, we demonstrated electricity generation in a single chamber MFC directly fed with CO (Mehta et al., 2010). The maximum volumetric power output and CO transformation efficiency of the systems were 6.4 mW L_R^{-1} and 53%, respectively, and although comparable with current literature, this was relatively low. Based on experimental observations, Mehta et al. (2010), suggested that the performance of a CO-fed MFC could be increased by adopting an efficient method for gas to liquid transfer, while optimizing the anodic chamber and avoiding CO related inhibition of electricigenic microorganisms.

For sparingly soluble gases such as CO, the primary resistance to transport is in the liquid side of the film at the gas–liquid interface (Bredwell et al., 1999; Riggs and Heindel, 2006). Membrane systems offer an efficient and relatively inexpensive method for gas–liquid mass transfer with reduced reactor volumes (Munasinghe and Khanal, 2010a; Scott and Hughes, 1996). Thin synthetic polymer membranes have been studied considerably for their mass transfer properties (Robb, 1968). Hence, either a dense polymer or

---

a micro-porous membrane could be employed in a MFC depending on the characteristics of the gas and operating conditions of the process. In a dense polymer membrane, the gas is absorbed into the polymer at high pressure and is carried into the liquid (lower pressure side) by diffusion across the membrane (Yasuda and Lamaze, 1972). In contrast, the gas in a micro-porous system is transported into the liquid through the pore system rather than through the polymer (Côté et al., 1989). Dense polymer membranes, such as silicone membranes, offer an advantage over micro-porous membranes as they can be operated under high pressure conditions, which increase the concentration gradient and hence, the mass transfer rate (Côté et al., 1989). Silicone membranes have been reported to be ideal for membrane based bubble-less aeration without vigorous mixing where a conventional system is unable to meet the O_2 requirements of a higher rate system (Ahmed and Semmens, 1992; Côté et al., 1989). They also find wide applicability in modified atmosphere storage for fruits and vegetables because of efficient regulation of the gas levels in the storage chamber due to their selective gas permeation properties (Gariépy et al., 1994). Though silicone membranes have not yet been extensively studied for CO transfer from gas to liquid, they have been reported to have much higher diffusion rates for gases in comparison to other hydro-carbon polymers (Robb, 1968). Therefore, it was hypothesized that silicone membranes could offer an efficient membrane based mass transfer system for CO.

The current study compares the silicone membrane and silicone tubing membrane for CO transfer to the anodic liquid and demonstrates MFC operation on CO and syngas CO at an improved volumetric power output.

2. Methods

2.1. Membrane systems for CO transfer

The silicone membrane (SSP LLC, NY, USA) used in this study consisted of a fine nylon fabric (52–54 g/m^2) calendered with a thin uniform layer of silicone rubber ($\sim$90 μm). The fabric enhanced the mechanical properties of the membrane, while the silicone rubber was responsible for its gas permeation properties. A silicone tubing (VWR International LLC, Radnor, PA, USA) with a wall thickness of 9 μm and an external diameter of 0.076 mm was used. The total surface area for the silicone membrane and the tubing used in the tests was kept constant at 50 cm^2.

2.2. Volumetric mass transfer coefficient (K_La) estimation

The experimental set-up for determination of K_La consisted of a 50 mL test chamber custom made (Wolltech, Montreal, Canada) from Makrolon (polycarbonate) plates filled with tap water (Figs. 1 and 2A). Silicone tubing wound around a support was placed directly inside the test chamber as shown in Fig. 1A. For the silicone membrane an extra plate serving as the CO compartment was attached to the test chamber with the membrane acting as a wall between the two compartments as shown is Fig. 2A. The inlet of the CO compartment or the silicone tubing was connected to a CO bag, while the outlet was connected to a manometer. Both, the CO compartment and the tubing were maintained at a constant pressure throughout the experiment.

K_La values for CO were determined using the method described by Munasinghe and Khanal. (2010b), introducing a step change in dissolved CO concentration and then evaluating the concentration as a function of time. For this condition, the desired CO flow rate was set using a peristaltic pump connected to a timer prior to the start of the experiment. A gas tight syringe was used to collect water samples from a sampling port in the liquid recirculation line

at regular intervals until the dissolved CO concentration reached a steady state. The dissolved CO concentration was determined as described by Lide and Frederickse (1995). The sampled liquid was transferred into a hermetically sealed vial and placed in a 90 °C water bath for 10 min in order to achieve equilibrium between the liquid and the gas phase. The gas in the headspace of the vial was then analyzed as described below.

The K_La value was estimated based upon the mass balance equation $dC/dt = K_La(C_{ct} - C_t)$ (Munasinghe and Khanal, 2010b), where C_t is the dissolved CO concentration at time t and C_{ct} is the CO concentration in equilibrium between the gas–liquid phase.

Assuming that C_{ct} is constant at all times, there is no chemical reaction, and initially (at $t = 0$) there is no gas present in the test chamber, the solution of the mass balance equation yields:

$$\ln\left(\frac{C_{ct} - C_o}{C_{ct} - C_t}\right) = (K_La)t \tag{1}$$

Where: C_o is the initial dissolved CO concentration.

Eq. (1) corresponds to a linear relationship, in which the slope of the line is the volumetric mass transfer coefficient, K_La (Munasinghe and Khanal, 2010b; Riggs and Heindel, 2006).

2.3. Medium composition, inoculum and analytical methods

The composition of the stock solution of nutrients in g/L was 1.87 NH_4Cl, 14.81 KCl, 6.40 K_2HPO_4, 4.07 KH_2PO_4 and 0.415 yeast extract. The trace metal stock solution was prepared according to Tartakovsky et al. (2008). The chemicals used were all of analytical grade. The stock solutions were sterilized and maintained at 4 °C until used. The MFC influent solution was prepared by adding 35 mL of the nutrient solution and 1 mL of the trace metal solution to 1 L of de-ionized water. This solution had a conductivity of 12 mS cm^{-1}. The MFC's were inoculated with 10 mL of anaerobic sludge obtained from a food processing plant (Lassonde Inc., Rougemont, QC, Canada). The sludge was stored at 4 °C, and the pH of the sludge was 6.8–7.0.

Acetate and other volatile fatty acids (VFAs) were analyzed in an Agilent 6890 gas chromatograph (Wilmington, DE, USA) equipped with a flame ionization detector. The method details are provided in Tartakovsky et al. (2008). The pH and conductivity of the effluent were measured periodically. The volume of inflow and outflow gas was measured using bubble counters connected to glass U-tubes and interfaced with a data acquisition system.

The gas composition (H_2, CO, CH_4, O_2, N_2, and CO_2) was measured using an Agilent 6890 gas chromatograph (Wilmington, DE, USA) coupled to a thermal conductivity detector. Three hundred microliter of headspace sample was injected into a 4.5 m × 2 mm I.D. carboxen 1000 packed column from Sigma–Aldrich (St. Louis, MO, USA). The column was heated at 60 °C for 7 min, then raised to 225 °C at a rate of 60 °C per minute and maintained for 6 min. Argon was used as carrier gas. The injector and detector were maintained at 125 and 150 °C respectively.

2.4. MFC design, operation and characterization

MFC tests were conducted in an experimental set-up similar to that employed for K_La measurements. The 50 mL anodic compartment contained the 5 mm thick graphite felt anode measuring 10 × 5 cm (Speer Canada, Kitchener, ON, Canada). A cathode was attached to one of the sides of the anodic compartment (Figs. 1 and 2B). All MFC tests were carried out using a carbon paper cathode containing 0.5 mg cm^{-2} Pt a catalyst, (GDE LT 120EW, E-TEK Division, PEMEAS Fuel Cell Technologies, Somerset, NJ, USA), which was separated from the anode by a piece of J-cloth, such that the estimated distance between the electrodes was 0.7–1 mm. The
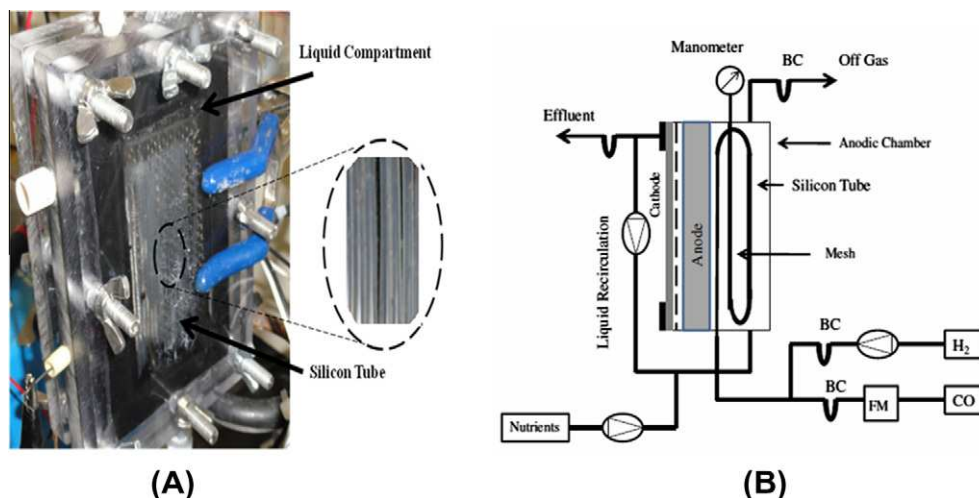
Fig. 1. (A) Experimental set-up for the determination of volumetric mass transfer co-efficient (K_La) for silicone tubing and (B) diagram of the experimental setup of silicone tubing incorporated MFC, where BC represents the bubble counters.
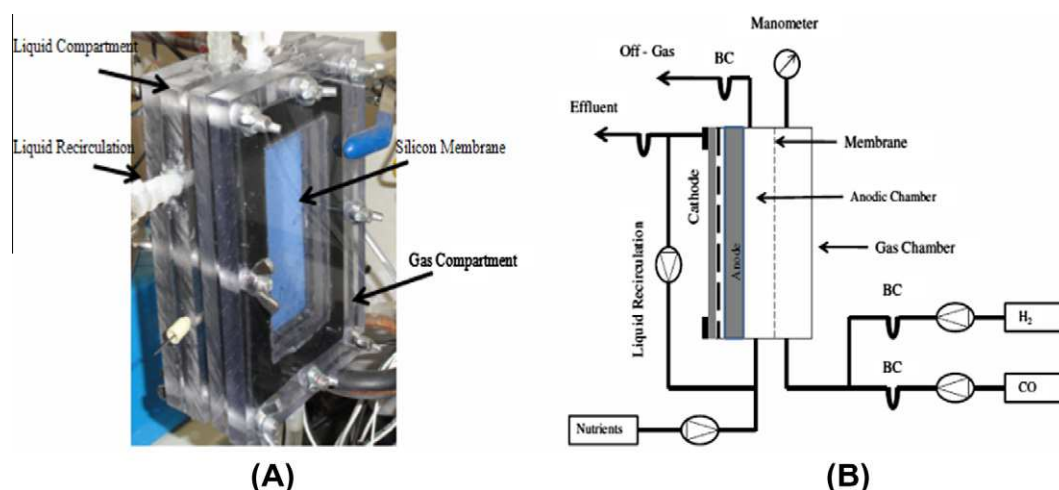

Fig. 2. (A) Experimental set-up for the determination of volumetric mass transfer coefficient (K_La) for silicone membrane and (B) diagram of the experimental setup of silicone membrane incorporated MFC, where BC represents the bubble counters.

cathode was prepared as described in Mehta et al. (2010). The MFC's were equipped with lines for influent, effluent, liquid recirculation, gas exit and entry as shown in Figs. 1 and 2B. Medium was prepared and fed to the MFC at a rate of 75 mL/day using peristaltic pump. The MFC's were operated at 33–35 °C by heating the re-circulating liquid. The temperature was monitored and controlled by means of a thermocouple placed in the anodic chamber and a temperature controller (Model JCR-33A, Shinko Technos Co., Ltd., Osaka, Japan).

For silicone membrane MFC a 10 L gas bag (Control Concepts Inc., Calgary, Alberta, Canada) was used for continuous supply of CO. In the silicone tubing tests, the line for gas entry was connected to a CO cylinder and the CO flow rate was controlled by a flow meter (Alicat Scientific, AZ, USA). Several CO flow rates were tested in order to estimate and maximize CO consumption efficiency. The gas flow rates are expressed in L of gas fed per L of anodic chamber volume per day ($L\ L_R^{-1}\ d^{-1}$). CO flow rates of 4 and 6 $L\ L_R^{-1}\ d^{-1}$ were tested for silicon membrane MFC and CO flow rates of 2, 3 and 4 $L\ L_R^{-1}\ d^{-1}$ were tested for silicon tubing MFC (Table 1). Each flow rate was tested for at least 7 days. In addition to CO tests, syngas operation was simulated by attaching a 10 L H_2 bag to the CO line. A flow rate of 4 $L\ L_R^{-1}\ d^{-1}$ was used for CO and H_2 into the silicone

membrane MFC and 3 $L\ L_R^{-1}\ d^{-1}$ was used for silicon tubing MFC (Table 1). The gas flow rates tested in this study were similar to that tested in the previous study (Mehta et al., 2010). This was done to allow for a direct comparison of the volumetric power output and CO transformation efficiency achieved for the MFCs in this study to that achieved for the sparger installed MFC (Mehta et al., 2010).

MFC voltage was measured on-line at 20 min intervals using a data acquisition system (Labjack U12, Labjack Corp., Lakewood, CO, USA). Polarization tests were carried out at the end of each test using the following method. First, the open circuit voltage (OCV) was measured by disconnecting external resistance for 30 min. The external resistance was re-connected and progressively decreased in 8–11 steps with an interval of 10 min between each step to allow for voltage stabilization. The 10 min intervals provided a steady state voltage, while avoiding significant changes in the carbon source concentration in the anodic liquid. Output voltage measurements were conducted at the end of each interval. The measurements were started at 5000 Ω and terminated at 10 Ω. These measurements were used to generate polarization (voltage vs. current density) and power (output power vs. current density) graphs (Logan, 2008; Mehta et al., 2010). The linear part of the

Table 1
Performance of silicone membrane and silicone tubing incorporated MFCs at different carbon monoxide flow rates.

Silicone Membrane											
Test	L $(L_R)^{-1} d^{-1}$	Power output mW/L_R P_{max}^{op}	Power output mW/L_R P_{max}^{pt}	R_{int} (Ω)	CO transformation (%)	Effluent acetate (mg/L)	H_2 (%)	CH_4 (%)	CO (%)	CE (%)	CO conc. (mg/L)
1	6	11.2	10.1	175	67.8 ± 2	46.2	4.8	15.3	62.5	7.0	9.2
2	4	19.3	18	85	74.2 ± 3.1	18.4	3.1	11.1	55.1	10.7	7.2
3[a]	4[a]	8	7	170	57.2 ± 4.4	34.7	22	11.5	44.5	6.8	7.1
Silicone Tube											
1	4	12.2	11.7	150	88 ± 2.3	74	4.7	9.4	39.3	9.3	9.1
2	3	14	13	75	92 ± 1	58	2.1	9.3	33.2	16.3	7.8
3	2	4	3.1	200	98.4 ± 1	6.1	5.3	15	12.5	7.0	3.1
4[a]	3[a]	6.3	8.1	130	41.4 ± 2.6	51.4	26	3.3	48.4	8.8	8.4

[a] Syngas test (CO and H_2 fed simultaneously at the indicated flow rate).

polarization curve produced was used to estimate the total internal resistance (Logan, 2008). The open circuit potentials for anode and cathode were measured using a standard Ag/Agcl electrode (0.222 V vs NHE).

The Coulombic efficiency (CE) of the MFC was estimated as (Mehta et al., 2010):

$$CE = \frac{I \cdot \Delta t \cdot M_{CO}}{F \cdot n (M_{CO,in} - M_{CO,out})} 100\% \qquad (2)$$

where I is the average measured current (A), Δt is the time interval during which current was measured (s), M_{CO} is the molecular weight of CO (g), F is the Faraday constant (C/mol), n is the number of electrons (electron/mol), $M_{CO,in}$ is the amount of CO supplied (g) to the MFC during Δt and $M_{CO,out}$ is the amount of CO (g) recovered in the off-gas line during Δt.

The absence of power generation from the nutrients present in the influent stream (i.e. yeast extract) has been demonstrated earlier (Mehta et al., 2010). A low voltage output of 3–4 mV (Rext = 500 Ω, Pout < 0.02 × 10^{-3} mW) was observed when the MFC was fed only with the solution of nutrients and microelements in the absence of CO-feeding for 1 week (Mehta et al., 2010). In this study, at start-up the MFCs were operated under a constant external resistance and comparatively low CO flow rate. Once a steady power output was observed, the CO flow rate was stepped up and the external resistance was optimized using the Perturbation and Observation MPPT algorithm (Woodward et al., 2009). The external optimized resistance using the online algorithm was always found to be within the range of 20 Ω to that of the internal resistance obtained from the polarization curves. The effluent and anodic off-gas compositions were analyzed periodically. In order to estimate the dissolved CO concentration levels corresponding to optimum performance, the dissolved CO concentration in the anodic liquid was measured regularly. At each tested flow rate, polarization tests were performed to estimate the MFC internal resistance and maximum power output (P_{max}^{pt}). Also, the average (P_{av}) and maximum operational power output (P_{max}^{op}) observed during the course of MFC operation at a particular CO flow rate is also reported. Notably, P_{av} takes into account the fluctuations in power output.

3. Results and discussion

3.1. Estimation of $K_L a$

The $K_L a$ values for CO were calculated using the analytical solution of the dissolved CO material balance (Eq. (1)). The silicone membrane and tubing were operated in a dead-end mode. This mode of operation allowed for an elevated gas pressure in the sys-

tem due to gas build up, which increased the concentration gradient and hence the mass transfer of CO (Ahmed and Semmens, 1992). The CO $K_L a$ for silicone membrane and tubing were estimated to be 0.63 ± 0.1 and 0.76 ± 0.2 h^{-1}, respectively. For an optimum performance of a CO-fed MFC, the rate of CO transfer needs to be matched to that of its consumption, since an excessive transfer would lead to CO-related inhibition of carboxydotrophic and electricigenic microorganisms (Henstra et al., 2007; Mehta et al., 2010; Sipma et al., 2006). The CO transfer rates obtained for the silicone membrane and silicone tubing sufficiently matched to the gas transfer requirements for the CO-fed MFC in the study of Mehta et al. (2010); confirming the feasibility of using silicone membrane and tubing for CO transfer in MFCs. The $K_L a$ value for silicone tubing was comparably higher than for the membrane, conceivably due to the difference in their thickness (Ahmed and Semmens, 1992). Comparable CO $K_L a$ in the range of 0.4–1.1 h^{-1} for composite hollow fiber membrane modules has been recently reported (Munasinghe and Khanal, 2010b). To our knowledge, no other literature evaluating the mass transfer of CO (gas to liquid) through membrane systems is currently available.

3.2. MFC tests

The operation of the silicone membrane MFC was started with a CO flow rate of 2 L L_R^{-1} d^{-1} and an external resistance of 1089 Ω. After a delay of 2 weeks, a steady voltage of 203 mV corresponding to a power output of 0.76 mW L_R^{-1} was observed. At this point, the CO flow rate was stepped up to 6 L L_R^{-1} d^{-1} and the external resistance was now optimized using the online optimization algorithm. After 9 days of operating the MFC at this flow rate, an average (P_{av}) and maximum operational power output P_{max}^{op} of 6 mW L_R^{-1} (Fig. 5A) and 11.2 mW L_R^{-1} (Table 1), respectively were observed. A maximum power output (P_{max}^{pt}) of 10.1 mW L_R^{-1} with an internal resistance of 175 Ω (Table 1) was estimated based on the polarization curves (Fig. 3). An open circuit voltage (OCV) value of 576 mV was observed with the cathode and anode OCP values lying in the range of 200 and 210 mV and between 350 and 385 mV, respectively. Flow rates higher than 6 L L_R^{-1} d^{-1} were not tested as it was found to impede the MFC output in our earlier study (Mehta et al., 2010). As mentioned earlier, for the optimum performance of a CO-fed MFC, the rate of gas transfer must match the rate of its consumption. The relatively high levels of dissolved CO concentration at higher CO flow rates leads to the inhibition of carboxydotrophic and electricigenic microorganisms, thereby impeding the performance of the MFC (Henstra et al., 2007; Mehta et al., 2010). Decreasing the CO flow rate to 4 L L_R^{-1} d^{-1} increased P_{av} and P_{max}^{op} to 8.4 mW L_R^{-1} (Fig. 5A) and 19.3 mW L_R^{-1} (Table 1), respectively. Also, the CO transformation efficiency of the system increased to 74.2% (Table 1). The P_{max}^{pt} increased to 18 mW L_R^{-1}
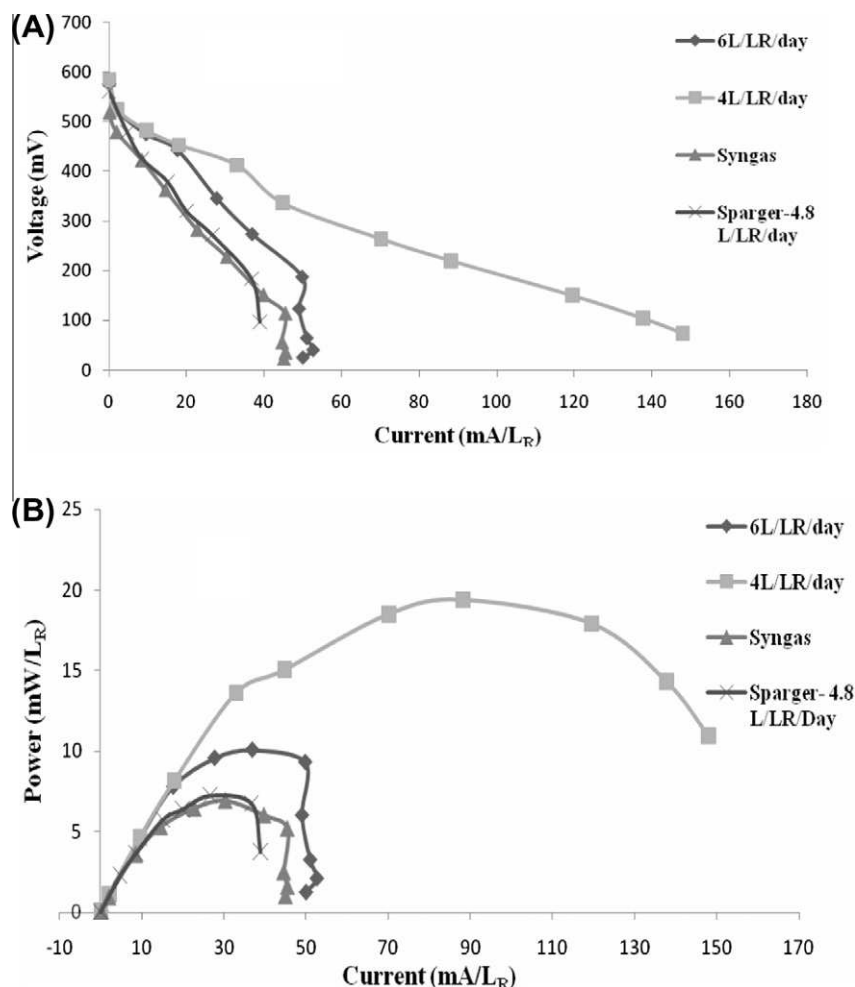
Fig. 3. Polarization (A) and power (B) curves obtained for silicone membrane incorporated MFC, where sparger represents the values obtained for the sparger installed MFC maximized at the flow rate of 4.8 L L_R^{-1} d^{-1} (Mehta et al., 2010).

(Fig. 3) and the internal resistance decreased to 80 Ω (Table 1). This increase in performance was plausibly due to a drop in dissolved CO concentration levels as given in Table 1.

As the maximum power output for silicone membrane MFC was observed at a CO flow rate of 4 L L_R^{-1} d^{-1}, the syngas test was performed by feeding both CO and H_2 at a flow rate of 4 L L_R^{-1} d^{-1}. After an initial drop of power output to 2 mW L_R^{-1}, the power output progressively increased to 10 mW L_R^{-1} within 4 days of starting of the syngas test. The anodic chamber had to be opened at this point due to technical problems, which resulted in exposure of the anode to oxygen. The MFC was restarted with syngas feeding and a recovery period of 1 week was required before any activity could be observed. The power output later increased to 8 mW L_R^{-1}. The performance of the MFC was plausibly hampered by the inhibition of the anaerobic carboxydotrophic and electricigenic microorganisms upon exposure to O_2, which was ascertained by a decrease in anode OCP to between 220–240 mV. Carboxydotrophs are strict anaerobes that are sensitive to O_2 (Oelgeschlager and Rother, 2008). A similar decrease in the output of a CO-fed MFC upon exposure of the anode to oxygen was also observed in our previous study (Neburchilov et al., 2011). Continued operation of the MFC on syngas for 15 days produced P_{max}^{pt} and P_{av} of 7 mW L_R^{-1} (Table 1) and 7.2 mW L_R^{-1} (Fig. 5A) respectively, which were approximately 65% higher than that previously reported for a syngas fed MFC (Mehta et al., 2010).

Notably, the fluctuations in the power output observed during the operation of silicone membrane MFC was likely caused by trace amounts of O_2 in the gas bags used to feed the MFC with CO and H_2. An increase in power output was always observed within 24 h of replenishing the gas bag. In order to obtain the best estimation of MFC performance the polarization tests were always performed within 24–30 h after replenishing the gas bags when the MFC performance was observed to be most stable.

In general, the performance of a silicone membrane MFC was comparatively better than that observed for the sparger equipped MFC in the previous study (Mehta et al., 2010). The maximum volumetric power outputs, P_{av} and P_{max}^{pt} at the CO flow rate of 4 L L_R^{-1} d^{-1} were approximately 35% and 180% higher than that previously reported (Kim and Chang, 2009; Mehta et al., 2010). Also, the CO transformation efficiency increased by 20%. The CE obtained during CO feeding was comparable to that reported for the sparger equipped MFC (Mehta et al., 2010).

For studying the performance of the silicone tubing MFC, a silicone tube wound around a support (stainless steel mesh) was placed next to the anode. Also, in order to avoid the problem of fluctuation in power output due to O_2 diffusion in the gas bags, the CO line was connected directly to a CO cylinder. The tests were performed with the same anode as that used in the silicone membrane tests, thus the variations in power output resulting from differences in the microbial populations were avoided.

The CO transformation efficiency in the silicon tubing MFC was comparatively higher than that observed for the silicone membrane MFC, with the maximum power outputs, P_{max}^{op} and P_{max}^{pt} observed at a CO flow rate of 3 L L_R^{-1} d^{-1} (Table 1). The P_{max}^{pt} and P_{av} were 13 mW L_R^{-1} (Fig. 4) and 10.3 mW L_R^{-1} (Fig. 5B) respectively, which were approximately 60% and 103% higher than that observed in previous study (Mehta et al., 2010). Also, a CO transformation efficiency of 92% was achieved (Table 1.) Though the maximum CO transformation efficiency of 98.5% (Table 1) was observed at a flow rate of 2 L L_R^{-1} d^{-1}, the power output (Fig. 4) was comparatively lower as the process was plausibly limited by low acetate concentrations. The electricity generation in a CO fed MFC predominantly takes place by the conversion of CO to acetate by the acetogenic carboxydotrophic microorganisms followed by the oxidation of acetate by CO tolerant electricigenic microorganisms. Low acetate levels at low CO flow rates limits electricity generation in a CO-fed MFC (Mehta et al., 2010).

Silicon tubing MFC operation on syngas was tested by feeding CO and H$_2$ at a flow rate of 3 L L_R^{-1} d^{-1}. A P_{max}^{pt} of 8.1 mW L_R^{-1} (Fig. 4) and a P_{av} of 6.7 mW L_R^{-1} (Fig. 5B) were observed, which were approximately 92% and 60% higher than that previously reported (Mehta et al., 2010). Fluctuations in power output of silicon tubing MFC were less intense than those observed for silicone membrane MFC. However, the O$_2$ levels in the anodic chamber of silicone tubing MFC increased with the installation of the H$_2$ bag, impeding the carboxydotrophic activity, which can be inferred from the low CO transformation efficiency (41.5%) and a decrease in anode OCP (250–270 mV) observed during the syngas test.

In general, the volumetric power output of silicone tubing MFC was comparable to that obtained for silicone membrane MFC, but the CO transformation efficiency for silicone tubing MFC was considerably higher due to better CO gas to liquid transfer capability of silicone tubing as reflected by the higher CO K$_L$a value for the tubing than for the silicone membrane. Consequently, the optimum level of dissolved CO was achieved at a lower CO flow rate. The power output was maximized at dissolved CO levels of 7.8–8 mg/L (Table 1).

The maximum current density achieved for silicone membrane and silicone tubing MFCs were in a range of 1.0–1.4 and 0.7–0.9 A m^{-2}, respectively. Acetate-fed MFCs have been reported to have a similar current density of 1.1–2.0 A m^{-2} and a power output of 10–100 mW L_R^{-1} (Logan et al., 2006; Lovley, 2008; Martin et al., 2010; Neburchilov et al., 2011; Pinto et al., 2010). Such current densities could be considered low for a hydrogen fuel cell, however they are sufficient to consider an MFC as a feasible technology for electricity production from organic waste (Logan, 2010). In our
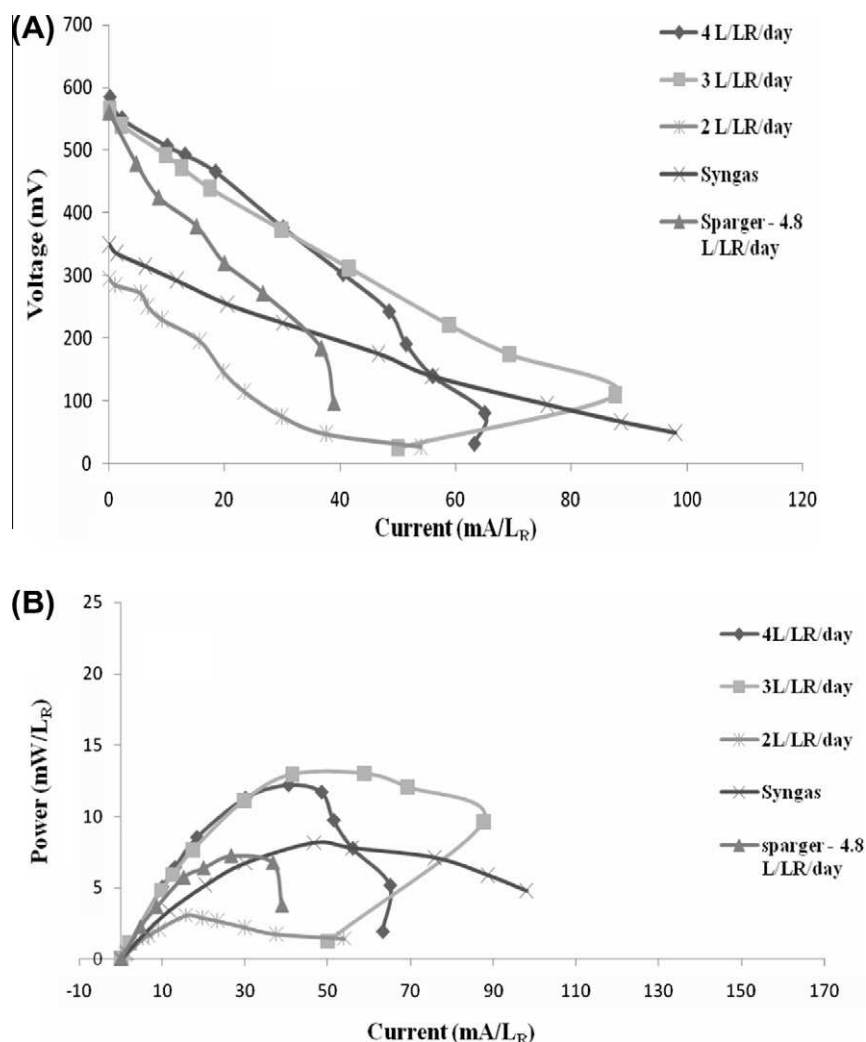

Fig. 4. Polarization (A) and power (B) curves obtained for silicone tubing incorporated MFC, where sparger represents the values obtained for the sparger installed MFC maximized at the flow rate of 4.8 L L_R^{-1} d^{-1} (Mehta et al., 2010).
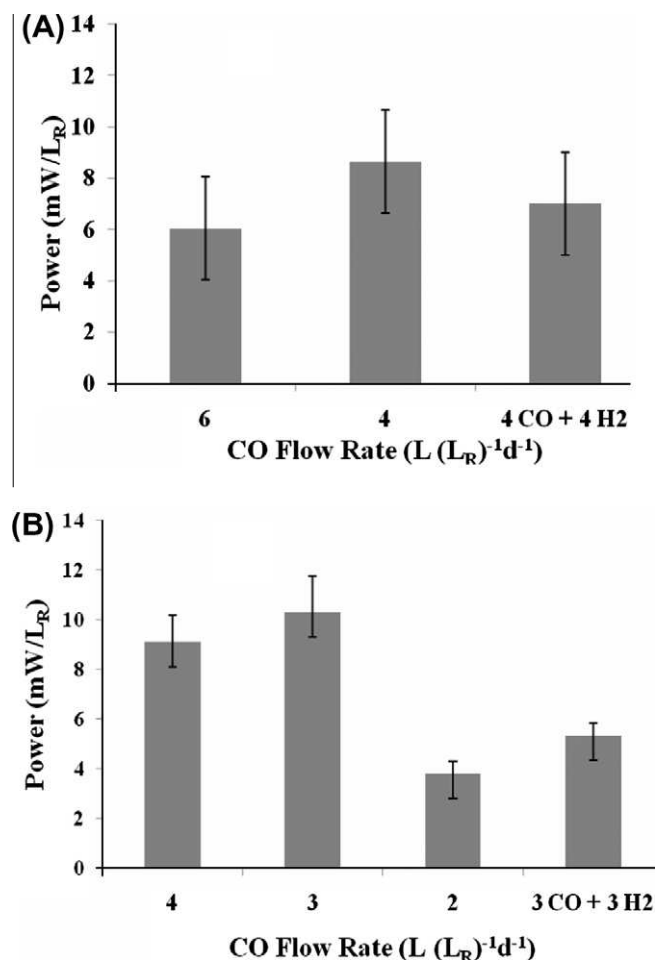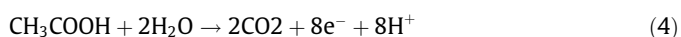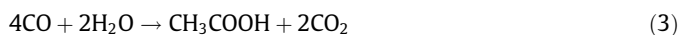
Fig. 5. Average volumetric power output for (A) silicone membrane and (B) silicone tubing incorporated MFCs at different CO flow rates. The error bars represent the calculated standard deviation for the data points.

study, the anode occupied 25 mL of the anodic chamber. By recalculating the volumetric power output per anode volume, a power output of 36 mW/L_{anode} for silicone membrane (at 4 L L_R^{-1} d^{-1}) and 26 mW/L_{anode} for silicone tubing (at 3 L L_R^{-1} d^{-1}) was obtained, which implies that further design improvements/optimization of cathode and the anodic chamber can result in a higher power output for a CO-fed MFC.

The results of VFA and off gas analysis (Fig. 6) for silicone membrane and silicone tubing tests were in accordance to previous observations (Kim and Chang, 2009; Mehta et al., 2010). The effluent measurements demonstrated the predominance of acetate as the major metabolite with propionate, methanol and ethanol were present only in trace amounts. The concentration of acetate increased as CO flow rate increased (Table 1). Degradation products such as H_2 and CH_4 were detected in the anode off-gas. Based on the analysis of metabolic products, Mehta et al. (2010) hypothesized that the production of electricity in CO-fed MFC proceeds through multi-step concurrent pathways. The conversion of CO to acetate followed by the oxidation of acetate by CO tolerant electricigenic microorganisms is hypothesized to be the most prominent pathway. The following stoichiometric equations describe this pathway (Mehta et al., 2010; Hussain et al., 2011):

$$4CO + 2H_2O \rightarrow CH_3COOH + 2CO_2 \tag{3}$$

$$CH_3COOH + 2H_2O \rightarrow 2CO2 + 8e^- + 8H^+ \tag{4}$$

The presence of H_2 in the off-gas when the MFC was operated on CO was indicative of hydrogenogenic activity. It was hypothesized that H_2 was used as an electron donor for electricity generation by the electricigenic microorganisms. Electricity generation in a MFC fed with H_2 has previously been demonstrated (Bond and Lovley, 2003). This particular pathway can be expected to have profound relevance for MFC operation on syngas. Finally, the possibility of direct electron transfer to the anode by recently isolated metal reducing carboxydotrophic micro-organisms was also discussed (Mehta et al., 2010).

Even though significant levels of acetate were observed in the anodic liquid, the CE of the system was invariably low, conceivably due to the concomitant production of CH_4 and other degradation products (Mehta et al., 2010; Sipma et al., 2003). In the study of Sipma et al. (2003) CO conversion in some cases led to the production of acetate and CO_2 and to CH_4 and CO_2 in others. More importantly it was noticed that acetate seemed to serve as the main intermediate for CH_4 production, implying that much higher CE for a CO-fed MFC can be achieved if the formation of CH_4, H_2 and other degradation products can be kept to a minimum. Mehta et al., (2010) reported a CE of 33% for a CO-fed MFC when the calculations were modified to take into account the consumption of fed CO for the production of CH_4, H_2 and acetate that was not used for electricity production. This CE is only marginally lower that reported for acetate MFCs with comparable designs (Logan, 2008).

Overall, the operation of a silicone membrane and silicone tubing MFCs clearly demonstrated that the performance of a CO-fed MFC can be significantly increased by adopting efficient mass transfer techniques. In our earlier study (Mehta et al., 2010), a sparger was used for gas to liquid transfer of CO. The installation of the sparger required not only the doubling of the anode compartment volume (100 mL) but also much higher CO flow rates to achieve the desired dissolved CO levels due to mass transfer limitations; resulting in considerable gas losses and a low CO transformation efficiency. In this study, with the installation of a silicone membrane or tubing, an efficient gas to liquid transfer was achieved with a reduced anodic volume (50 mL), which considerably increased the volumetric power output along with a significant increase in CO transformation efficiency.

Interestingly, we observed biofilm formation on the surface of silicone membrane (facing the liquid) and also on the tubing. Biofilm formation on membrane surfaces has been widely reported. In the patent held by Hickey et al. (2008) a membrane bioreactor was employed for the conversion of CO or syngas to ethanol and other liquid products. The membrane concurrently served as support for biofilm growth. Biofilm formation on the surface of silicone membranes in membrane bioreactors for waste gas and water treatment has been reported (Kumar et al., 2008; Reij et al., 1998). This phenomenon of biofilm formation on silicone membrane surfaces is quite pertinent to CO-fed MFCs, where a biofilm formation on membrane surface would increase the density of acetogenic carboxydotrophic microorganisms in the anodic chamber and thereby increasing the acetate concentration and CO transformation efficiency.

CO and syngas fed MFCs offer a promising technology that has a number of advantages over polymer electrolyte membrane fuel cells (PEMFC) or solid oxide fuel cells (SOFC), as MFCs do not require noble catalysts at the anode nor are they very sensitive to fuel impurities as it has been previously reported in the case of PEMFC and SOFC (Kim and Chang, 2009; Song, 2002). The MFC based process can be used to combine electricity production with hydrogen extraction from syngas or in combination with syngas biotransformation to valuable energy carriers, such as butanol (Pengmei et al., 2007).
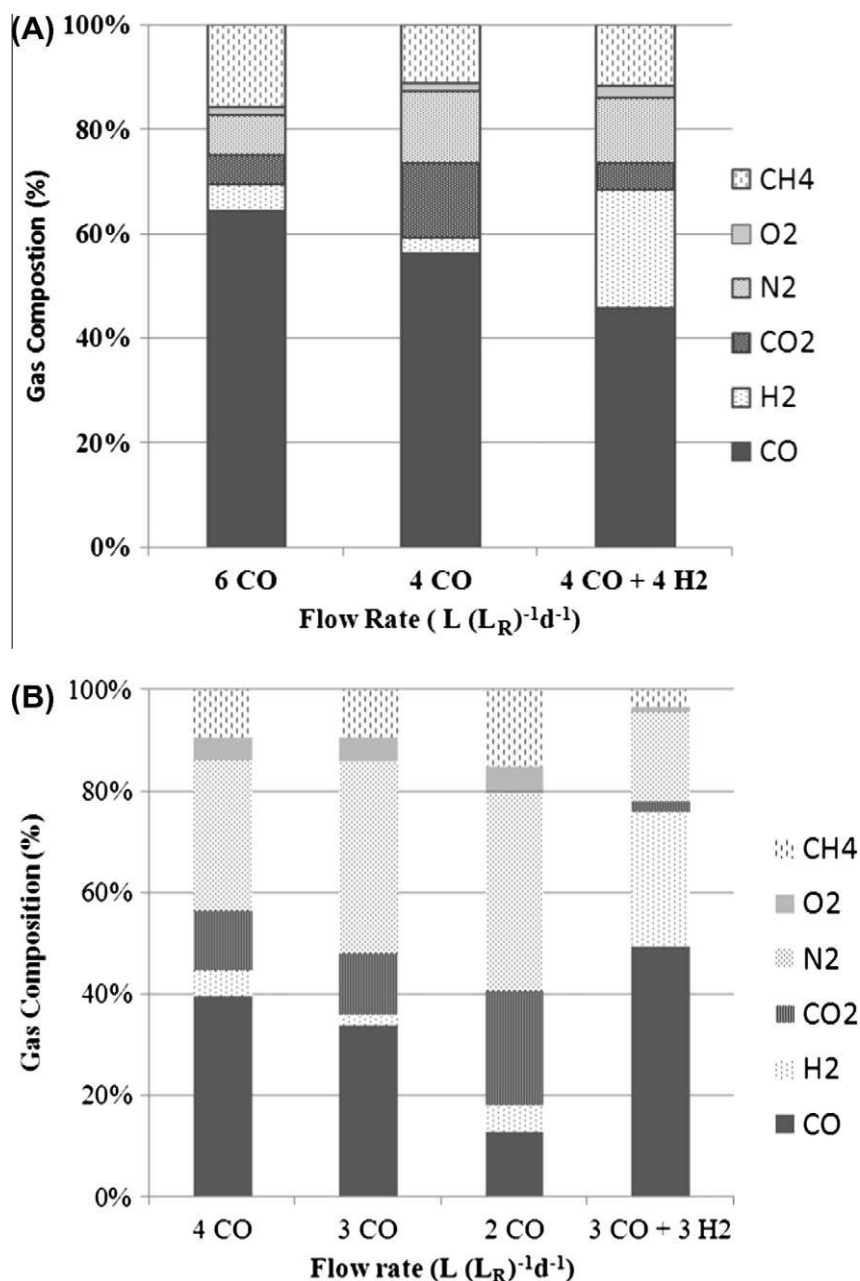
Fig. 6. Anodic off–gas composition for (A) silicone membrane and (B) silicon tubing incorporated MFC.

4. Conclusion

This study demonstrated the feasibility of using dense polymer membranes such as silicone membranes and thin wall silicone tubing, for efficient mass transfer of CO into a MFC. Thin silicone membranes and tubing can be easily incorporated into a MFC without requiring extensive changes in its design. A P_{max}^{pt} of 13 mW L_R^{-1} and 18 mW L_R^{-1} was achieved in silicone tubing and membrane installed MFC respectively, which was approximately 103% and 180% higher than that previously reported. Also, much higher CO transformation efficiencies in the range of 75–99% were obtained. Future studies might focus on testing other gas diffusion membranes with a high affinity for CO. Improved gas transfer demonstrated by the membrane-based systems, allows for focusing on the process microbiology, which could lead to the isolation of novel electricigenic carboxidotrophic microorganisms.

References

Ahmed, T., Semmens, M.J., 1992. Use of sealed end hollow fibers for bubbleless membrane aeration: experimental studies. J. Membrane Sci. 69, 1–10.
Bond, D.R., Lovley, D.R., 2003. Electricity production by *Geobacter sulfurreducens* attached to electrodes. Appl. Environ. Microbiol. 69, 1548–1555.
Bredwell, M.D., Srivastava, P., Worden, R.M., 1999. Reactor design issues for synthesis-gas fermentations. Biotechnol. Progr. 15, 834–844.
Bridgwater, T., 2006. Biomass for energy. J. Sci. Food Agriculture 86, 1755–1768.
Côté, P., Bersillon, J.-L., Huyard, A., 1989. Bubble-free aeration using membranes: mass transfer analysis. J. Membrane Sci. 47, 91–106.

Gariépy, Y., Raghavan, G.S.V., Munroe, J.A., 1994. Long-term storage of leek stalks under regular and controlled atmospheres. Int. J. Refrig. 17, 140–144.

Henstra, A., Sipma, J., Rinzema, A., Stams, J., 2007. Microbiology of synthesis gas fermentation for biofuel production. Curr. Opin. Biotechnol. 18, 200–206.

Hickey, R., Datta, R., Tsai, s.-P., Basu, R., 2008. Memrane supported bioreactor for conversion of syngas components to liquid products, (Ed.) U.S.P. Publication, vol. US 200/0305539 A1. US, pp. 1–5.

Hussain, A., Guiot, S., Mehta, P., Raghavan, V., Tartakovsky, B., 2011. Electricity generation from carbon monoxide and syngas in a microbial fuel cell. Appl. Microbiol. Biotechnol. 90, 827–836.

Kim, D., Chang, I.S., 2009. Electricity generation from synthesis gas by microbial processes: CO fermentation and microbial fuel cell technology. Bioresource Technol. 100, 4527–4530.

Kumar, A., Dewulf, J., Van Langenhove, H., 2008. Membrane-based biological waste gas treatment. Chem. Eng. J. 136, 82–91.

Lide, D.R., Frederickse, H.P.R., 1995. Handbook of Chemistry and Physics, seventy sixth ed. CRC Press Inc., Boca Raton, FL.

Logan, B., 2010. Scaling up microbial fuel cells and other bioelectrochemical systems. Appl. Microbiol. Biotechnol. 85, 1665–1671.

Logan, B.E., 2008. Microbial Fuel Cells. John Wiley & Sons Inc, Hoboken, NJ.

Logan, B.E., Hamelers, B., Rozendal, R., Schröder, U., Keller, J., Freguia, S., Aelterman, P., Verstraete, W., Rabaey, K., 2006. Microbial Fuel Cells: methodology and Technology†. Environ. Sci. Technol. 40, 5181–5192.

Lovley, D.R., 2008. The microbe electric: conversion of organic matter to electricity. Curr. Opin. Biotechnol. 19, 564–571.

Martin, E., Savadogo, O., Guiot, S.R., Tartakovsky, B., 2010. The influence of operational conditions on the performance of a microbial fuel cell seeded with mesophilic anaerobic sludge. Biochem. Eng. J. 51, 132–139.

Mehta, P., Hussain, A., Raghavan, V., Neburchilov, V., Wang, H., Tartakovsky, B., Guit, S., 2010. Electricity generation from a carbon monoxide in a single chamber microbial fuel cell. Enzyme Microb. Technol. 46, 450–455.

Munasinghe, P.C., Khanal, S.K., 2010a. Biomass-derived syngas fermentation into biofuels: opportunities and challenges. Bioresource Technol. 101, 5013–5022.

Munasinghe, P.C., Khanal, S.K., 2010b. Syngas fermentation to biofuel: evaluation of carbon monoxide mass transfer coefficient (k_La) in different reactor configurations. Biotechnol. Progr. 26, 1616–1621.

Neburchilov, V., Mehta, P., Hussain, A., Wang, H., Guit, S., Tartakovsky, B., 2011. Microbial fuel cell operation on carbon monoxide: cathode catalyst selection. Int. J. Hydrogen Energ..

Oelgeschlager, E., Rother, M., 2008. Carbon monoxide - dependant energy metabolism in anaerobic bacteria and archaea. Arch. Microbiol. 190, 257–269.

Pengmei, L., Yuan, Z., Wu, C., Ma, L., Chen, Y., Tsubaki, N., 2007. Bio-syngas production from biomass catalytic gasification. Energ. Convers. Manage. 48, 1132–1139.

Pinto, R.P., Srinivasan, B., Manuel, M.F., Tartakovsky, B., 2010. A two-population bio-electrochemical model of a microbial fuel cell. Bioresource Technol. 101, 5256–5265.

Reij, M.W., Keurentjes, J.T.F., Hartmans, S., 1998. Membrane bioreactors for waste gas treatment. J. Biotechnol. 59, 155–167.

Riggs, S.S., Heindel, T.J., 2006. Measuring carbon monoxide gas–liquid mass transfer in a stirred tank reactor for syngas fermentation. Biotechnol. Progr. 22, 903–906.

Robb, W.L., 1968. Thin silicon membranes-their permeation properties and some applications. Ann. NY. Acad. Sci. 146, 119–137.

Scott, K., Hughes, R., 1996. Industrial Membrane Separation Technology. Blackie Academic & Professional, Glasgow, UK.

Sipma, J., Henstra, A.M., Parshina, S.N., Lens, P.N.L., Lettinga, G., Stams, A.J.M., 2006. Microbial CO conversions with applications in synthesis gas purification and bio-desulfurization. Cr. Rev. Biotechnol. 26, 41–65.

Sipma, J., Lens, P.N.L., Stams, A.J.M., Lettinga, G., 2003. Carbon monoxide conversion by anaerobic bioreactor sludges. FEMS Microbiol. Ecol. 44, 271–277.

Song, C., 2002. Fuel processing for low-temperature and high-temperature fuel cells: challenges, and opportunities for sustainable development in the 21st century. Catal. Today 77, 17–49.

Tartakovsky, B., Manuel, M.F., Neburchilov, V., Wang, H., Guiot, S.R., 2008. Biocatalyzed hydrogen production in a continuous flow microbial fuel cell with a gas phase cathode. J. Power Sources 182, 291–297.

Woodward, L., Tartakovsky, B., Perrier, M., Srinivasan, B., 2009. Maximizing power production in a stack of microbial fuel cells using multiunit optimization method. Biotechnol. Progr. 25, 676–682.

Yasuda, H., Lamaze, C.E., 1972. Transfer of gas to dissolved oxygen in water via porous and nonporous polymer membranes. J. Appl. Polym. Sci. 16, 595–601.